J. Fluid Mech. (2002), *vol.* 458, *pp.* 379–406.
DOI: 10.1017/S0022112002007930 Printed in the United Kingdom

The drainage of a foam lamella

By C. J. W. BREWARD[1] AND P. D. HOWELL[2]†

[1]Mathematical Institute, University of Oxford, 24–29 St Giles, Oxford OX1 3LB, UK

[2]School of Mathematical Sciences, University of Nottingham, University Park, Nottingham NG7 2RD, UK

(Received 9 August 2001 and in revised form 1 November 2001)

We present a mathematical model for the drainage of a surfactant-stabilized foam lamella, including capillary, Marangoni and viscous effects and allowing for diffusion, advection and adsorption of the surfactant molecules. We use the slender geometry of a lamella to formulate the model in the thin-film limit and perform an asymptotic decomposition of the liquid domain into a capillary-static Plateau border, a time-dependent thin film and a transition region between the two. By solving a quasi-steady boundary-value problem in the transition region, we obtain the flux of liquid from the lamella into the Plateau border and thus are able to determine the rate at which the lamella drains.

Our method is illustrated initially in the surfactant-free case. Numerical results are presented for three particular parameter regimes of interest when surfactant is present. Both monotonic profiles and those exhibiting a dimple near the Plateau border are found, the latter having been previously observed in experiments. The velocity field may be uniform across the lamella or of parabolic Poiseuille type, with fluid either driven out along the centreline and back along the free surfaces or vice versa. We find that diffusion may be negligible for a typical real surfactant, although this does not lead to a reduction in order because of the inherently diffusive nature of the fluid–surfactant interaction. Finally, we obtain the surprising result that the flux of liquid from the lamella into the Plateau border increases as the lamella thins, approaching infinity at a finite lamella thickness.

1. Introduction

A foam is a gas–liquid mixture in which the liquid phase is connected but has a small volume fraction. Foam is broadly classed as wet or dry, depending on the liquid content. In a wet foam (with a liquid volume fraction of 10–20%), the bubbles are approximately spherical, whereas a dry foam (in which the fraction of liquid is less than 10%) consists of roughly polyhedral bubbles. The thin liquid films forming the faces of the polyhedra are called lamellae and the tubes of liquid at the junctions of the lamellae (i.e. along the edges of the polyhedra) are called Plateau borders, after Plateau (1873). The vertices, where typically four Plateau borders meet, are referred to as nodes.

A two-dimensional slice through the edge of a lamella is shown schematically in figure 1. The curvature of the gas–liquid interface causes the liquid pressure to be lower in the Plateau border than in the lamella. The resulting Plateau border suction

† Present address: Mathematical Institute, University of Oxford, 24–29 St Giles, Oxford OX1 3LB, UK.

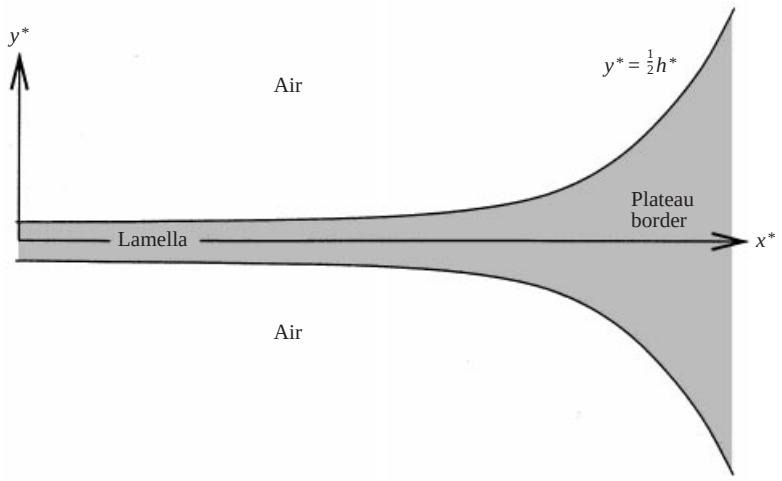

FIGURE 1. Schematic of the edge of a lamella.

drives a flux of liquid from the lamella into the Plateau border. If there is nothing to oppose this suction, then the lamella rapidly thins until it eventually becomes unstable and ruptures. For this reason, foam consisting of pure liquid (e.g. pure water) is relatively short-lived. One way in which its lifetime may be significantly extended is through the addition of a surface-active agent, otherwise known as a surfactant.

Surfactant molecules prefer to reside at a gas–liquid interface rather than in the bulk (Adamson 1982) and adsorption of surfactant in this manner reduces the surface tension of the interface (Atkins 1999). Non-uniform adsorption due, for example, to surface dilatation may therefore result in a surface tension gradient (Manning-Benson, Bain & Darton 1997; Bain, Manning-Benson & Darton 2000). This in turn leads to a so-called Marangoni shear stress acting on the liquid at the interface, and hence the flow is accelerated or retarded, depending on the direction of the gradient relative to the bulk liquid flow. This effect tends to stabilize a lamella if the surface shear opposes the Plateau border suction and, conversely, has a destabilizing influence if the Marangoni stress enhances the Plateau border suction.

Allowed to drain in a controlled environment, a lamella may become so thin that intermolecular forces arising from the interaction between the two free surfaces come into play. These forces, if repulsive, can balance capillary suction, resulting in a stable black film, of thickness 10^{-9}–10^{-8} m. A lamella may also be stabilized by the formation of a solid surface layer, for example in an ageing soap film. Neither of these mechanisms will be considered here; our concern is with a fundamentally unstable film, whose lifetime may nevertheless be extended considerably by Marangoni stresses caused by the presence of surfactant. As indicated in figure 1, we focus on the edge of a single lamella. Our aim is to predict the flux of liquid sucked into the neighbouring Plateau border and, thus, the rate at which the lamella thins. This process is fundamental to lamella rupture and, therefore, to bubble coalescence and foam collapse.

Experimental work on *in situ* foam lamellae remains sparse owing to the difficulties inherent in probing a foam. However, some work has been carried out on isolated liquid films. For example, Joye, Miller & Hirasaki (1992) present interference patterns from a single lamella containing surfactant above the critical micelle concentration (the

concentration at which surfactant molecules associate in the bulk to form micelles). Their results support the notion that such films exhibit a dimple close to the Plateau border, as do their numerical solutions of a simple heuristic model. Experiments have also been carried out on individual liquid films to determine their internal pressure and also to drain the liquid from the films mechanically; see Shugai (1998) for more details and a literature review.

Many authors have attempted to model lamella drainage. Several have followed an approach analogous to ours, namely decomposition of the film into various regions which are then matched or patched together. Schwartz & Princen (1987) consider four regions: a Plateau border, a transition region, a laid-down film and a black film. They apply a no-slip boundary condition, under the assumption that the gas–liquid interface is 'loaded with surfactant'. The resulting lubrication-style differential equation is solved under matching conditions with the Plateau border and with the laid-down film. Barigou & Davidson (1994) also decompose the liquid into four regions: a border region, two transition regions and a lamella. They treat the Plateau border as immobile and the lamella as free – the converse of the Schwartz & Princen conjecture. Again, the result is a lubrication-style equation, which is combined with heuristic shear and mass balances to estimate the lamella thinning rate. They also discuss the possibility of a sharp border contraction, corresponding to the dimpled effect at the edge of the lamella inferred by Joye *et al.* (1992), and conclude that the pressure distribution in such a configuration is 'physically impossible'.

Braun, Snow & Pernisz (1999) model a vertical film draining under gravity, including viscous and capillary effects. They also assume that the free surface is loaded with surfactant and so employ the no-slip boundary condition. The resulting time-dependent lubrication equation is matched with a hydrostatic meniscus, close to which numerical solutions exhibit dimples. Naire, Braun & Snow (2000*a*, *b*) replace the no-slip assumption with a surface viscosity and include a Marangoni stress induced by an insoluble surfactant. They show that increasing the surface viscosity slows down the film drainage and that, in the limit of high viscosity, the no-slip boundary condition is recovered. The materials in which we are interested have negligible surface viscosity so the surface traction can be adequately described using a Marangoni stress.

Many previous authors have used a long-wave asymptotic limit to obtain quasi-one-dimensional models for thin unsupported liquid films. For example, Ting & Keller (1990) consider pure inviscid liquid sheets, whereas Howell (1996) derives models for pure viscous sheets; Erneux & Davis (1993) and De Wit, Gallez & Christov (1994) include van der Waals forces, and the effects of insoluble surfactant are incorporated by Ida & Miksis (1998*a*, *b*). The governing equations stated in § 2 represent an analogous limit of the underlying Navier–Stokes, advection–diffusion and appropriate free-surface equations; a brief derivation may be found in Breward *et al.* (1997) and further details in Breward (1999). As in Barigou & Davidson (1994) and Schwartz & Princen (1987), our approach is to decompose the liquid into various domains, in which different asymptotic regimes prevail. Our model differs from all of these previous attempts to model lamella drainage because we include the effects of surfactant solubility and we adopt a systematic asymptotic matching approach.

In § 2, we present the thin-film equations describing the evolution of the film thickness, the liquid velocity and the concentration of surfactant. In § 3, we use the simplified problem of surfactant-free drainage to illustrate our domain decomposition. An analogous decomposition is then applied to surfactant-stabilized drainage in § 4, resulting in a quasi-steady boundary-value problem, whose properties are explored analytically. Numerical solutions for three particular parameter regimes of interest

are presented in § 5. Of particular interest is the observation that the flux of liquid from the lamella into the Plateau border increases as the lamella thins, sometimes appearing to approach infinity at a finite lamella thickness. We explore this possibility using asymptotic analysis in § 6. Finally, in § 7 we summarize our conclusions and discuss extensions to this work.

2. The mathematical model

2.1. *Thin-film equations*

We consider the two-dimensional geometry shown in figure 1, with coordinates x^* pointing along the centreline of the lamella, y^* in the transverse direction and t^* denoting time. The centreline of the lamella is assumed to be flat, since centreline curvature may be shown to decouple from the flow equations derived below, so long as the radius of curvature is small compared with the film thickness (Breward 1999). The liquid velocity and pressure are denoted by $\boldsymbol{u}^* = (u^*, v^*)^T$ and p^*, respectively, and the lamella thickness by h^*, so that the two free surfaces are given by $y^* = \pm\frac{1}{2}h^*(x,t)$. The liquid density ρ and shear viscosity μ are assumed to be constant, and the surface tension $\gamma^*(x,t)$ to be equal on the two interfaces – see Breward (1999) for generalizations. Finally, the liquid velocity is characterized by a typical value U, and the lamella geometry by a typical initial thickness h_0 and length L.

The Navier–Stokes equations and the usual free-surface conditions are non-dimensionalized as follows:

$$\left.\begin{array}{ll} (x^*, y^*) = L(x, \epsilon y), & t^* = (L/U)t, \\ (u^*, v^*) = U(u, \epsilon v), & p^* = (\mu U/L)p, \\ h^* = h_0 h, & \gamma^* = \gamma + (\Delta\gamma)\sigma(x,t). \end{array}\right\} \tag{2.1}$$

Here, γ is the surface tension of the pure liquid, and $\gamma - \Delta\gamma$ is the surface tension of a stationary surface of the surfactant solution in equilibrium (on which $\sigma = -1$). Note that frequently $\Delta\gamma \ll \gamma$. We relate $\Delta\gamma$ to material properties of the surfactant at the end of § 2.2. The dimensionless groups in the problem are the slenderness parameter, Reynolds number, capillary number and Marangoni number, given respectively by

$$\epsilon = \frac{h_0}{L}, \quad Re = \frac{\rho L U}{\mu}, \quad Ca = \frac{\mu U}{\gamma}, \quad Ma = \frac{\Delta\gamma}{\mu U}.$$

The thin-film equations are obtained by taking the asymptotic limit $\epsilon \to 0$. In doing so, it is usually necessary to take a view on the size of the other three dimensionless parameters compared to ϵ. However, we do not in advance know the correct scaling for the liquid velocity U; in fact, the velocity at which liquid flows out of the lamella is an important prediction of our model. The only assumption we can make with any certainty is that the Reynolds number is small, so that inertia may be neglected, at the velocities of interest. It then transpires (see Breward 1999) that there are two distinguished limits of the thin-film equations. In the first, there is a balance between extensional viscous, capillary and Marangoni effects, with a plug flow velocity profile (to leading order), whereas in the second, capillary and Marangoni effects balance and the velocity profile is parabolic. Since, as noted above, the velocity scaling U is unknown *a priori*, we present the following master equations which contain both distinguished limits (and hence all the other possible parameter regimes). To derive these equations, we use the following procedure. First, we pick the size of the capillary and Marangoni numbers. Then we derive, from the governing equations and boundary conditions, the appropriate thin-film equations corresponding to this choice of *Ma*

and Ca. We carry out this process for all values of Ca and Ma corresponding to distinguished asymptotic limits, and then combine all the resulting equations into the master equations presented below. The details of the calculations may be found in Breward (1999).

The thin-film equations comprise a pair of coupled nonlinear partial differential equations for the film thickness h and the cross-sectionally averaged longitudinal velocity, $\bar{u}(x,t)$:

$$h_t + (\bar{u}h)_x = 0, \tag{2.2}$$

$$(4h\bar{u}_x)_x + \frac{\epsilon}{2Ca}hh_{xxx} + \frac{2Ma}{\epsilon}\sigma_x = 0, \tag{2.3}$$

where u is related to $\bar{u}$ by

$$u = \bar{u} + \frac{\epsilon^3}{4Ca}h_{xxx}\left(\frac{h^2}{12} - y^2\right), \tag{2.4}$$

and the pressure reads

$$p = -2\bar{u}_x - \frac{\epsilon}{2Ca}h_{xx}. \tag{2.5}$$

Equations (2.2) and (2.3) represent conservation of mass and a longitudinal force balance, respectively. In (2.3), the first term represents extensional (viscous) forces, the second, capillary forces, and the third, Marangoni forces.

Notice that the two distinguished limits are (i) $Ca = O(\epsilon)$ and $Ma = O(\epsilon)$, when the first two terms in (2.3) balance and $u = \bar{u}$ to lowest order; (ii) $Ca = O(\epsilon^3)$ and $Ma = O(\epsilon^{-1})$, when (2.4) gives a parabolic flow profile and the second term in (2.3) necessarily dominates the first. The system (2.2)–(2.3) is closed by specifying the surface tension variation σ, which depends crucially on the local concentration of surfactant.

2.2. *Surfactant modelling*

For a soluble surfactant, we must distinguish between surfactant molecules in solution, at a bulk concentration C^* (mol m^{-3}), and those that are adsorbed in the surface, with surface concentration Γ^* (mol m^{-2}); see Chang & Franses (1995). Assuming they are in thermodynamic equilibrium, there is a functional relationship between Γ^* and C^* at the free surfaces. (Note that the assumption of thermodynamic equilibrium requires that the time scales for adsorption and desorption of surfactant at the free surface be much smaller than the drainage time scale used in this problem. We put bounds on the time scale associated with adsorption and desorption in § 4.1.) At reasonably low surfactant concentration this may be linearized to give the Henry isotherm $\Gamma^* = \eta C^*$ (Chang & Franses 1995), for some material constant η with the dimensions of length. Surfactant in solution is transported by convection and diffusion, with constant bulk diffusivity D. The adsorption of surfactant into the free surface is balanced by diffusive flux from the bulk, and adsorbed molecules are transported by convection in the interface. We neglect surface diffusion in this paper for simplicity. We shall see later that the various phenomena that we have included work together to produce a diffusion-like effect, in keeping with the findings of Breward *et al.* (2001) and Howell & Breward (2002).

The convection–diffusion equation for the bulk concentration and the associated boundary conditions are non-dimensionalized using

$$C^* = C_0 C, \quad \Gamma^* = \eta C_0 \Gamma,$$

where C_0 is a typical bulk surfactant concentration. The dimensionless groups that emerge are the Péclet number and the replenishment number, given respectively by

$$Pe = \frac{UL}{D}, \quad S = \frac{D}{U\eta}.$$

Again, we formulate a thin-film simplification of the governing equations in the limit $\epsilon \to 0$. Under the assumption that $\epsilon^2 Pe \ll 1$ (the so-called well-mixed approximation), the bulk concentration is uniform across the film, i.e. $C = C(x,t)$, and satisfies

$$(hC_x)_x - Peh(C_t + \bar{u}C_x) - \frac{2}{\epsilon S}(C_t + (u_s C)_x) = 0. \tag{2.6}$$

The three terms in (2.6) represent successively bulk diffusion, bulk convection and surface convection. In the final term, u_s is the surface velocity given, using (2.4), by

$$u_s = \bar{u} - \frac{\epsilon^3}{24Ca} h^2 h_{xxx}. \tag{2.7}$$

The final coupling between (2.6) and the thin-film equations (2.2) and (2.3) arises from the equation of state relating the surface tension to the surface concentration. Again, at reasonably low concentration the relation is approximately linear, so we set

$$\gamma^* = \gamma + \left(\frac{\mathrm{d}\gamma^*}{\mathrm{d}\Gamma^*}\right)\Gamma^*,$$

where $(\mathrm{d}\gamma^*/\mathrm{d}\Gamma^*)$ is a negative constant. We may then choose the unknown quantity $\Delta\gamma$ in the Marangoni number to be

$$\Delta\gamma = -\eta C_0 \left(\frac{\mathrm{d}\gamma^*}{\mathrm{d}\Gamma^*}\right),$$

and it follows that

$$\sigma = -C. \tag{2.8}$$

With (2.4) and (2.8), (2.2), (2.3) and (2.6) constitute a closed system for h, $\bar{u}$ and C.

3. Surfactant-free drainage

3.1. *Domain decomposition*

In this section, we illustrate our solution procedure by addressing the surfactant-free problem. This corresponds to setting $C = \Gamma = \sigma = 0$, so only (2.2) and (2.3) remain to be solved. We show the liquid domain under consideration in figure 2. Our first modelling assumption is that the velocity of the liquid in the Plateau border is small enough that we may treat the Plateau border as capillary-static. Thus, its free surfaces have constant mean curvature which, in our two-dimensional geometry, implies that they must be circular arcs of constant radius a. These intersect tangentially at three points, the points where the lamellae meet the Plateau border. For bubbles of a given size, the radius a is determined by the liquid fraction in the foam.

In the lamella, the free surfaces are almost flat and here we suppose that capillary effects are negligible. Near to the Plateau border, however, this assumption must break down, because the curvature of the film has to increase from practically zero to $O(1/a)$ to match into the Plateau border. In this transition region, capillary and viscous forces are both important, and the correct velocity scaling is selected by ensuring that they balance. Our procedure, therefore, is to decompose the liquid

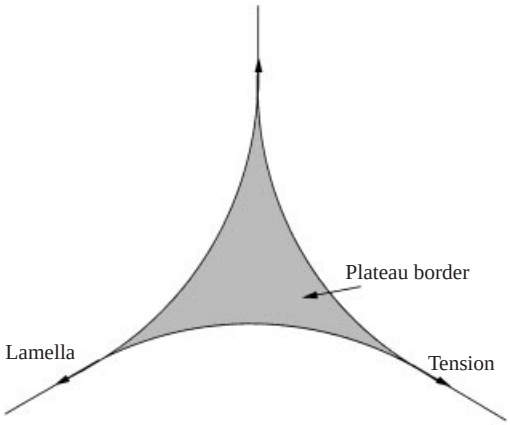

FIGURE 2. The outer picture.

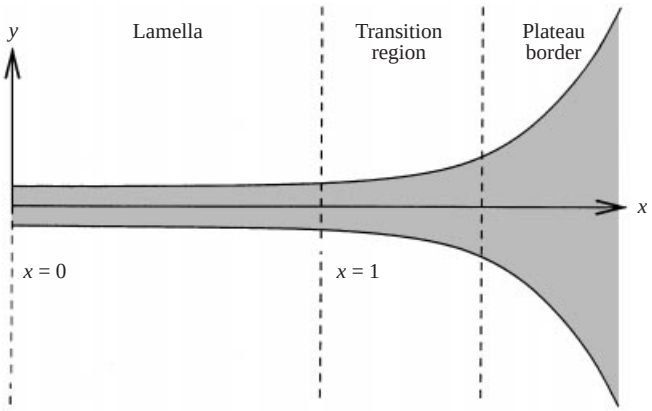

FIGURE 3. The inner picture.

domain into (i) a viscous lamella, (ii) a capillary-static Plateau border, and (iii) a transition region between the two in which viscous and capillary forces balance; see figure 3. An analogous decomposition was used by Howell (1999) to describe the drainage of a bubble at the surface of a bath of liquid.

The transition region has to match with the lamella, of typical thickness h_0, and with the curvature $1/a$ in the Plateau border, i.e., $h^* \to h_0$ as we approach the lamella, whereas $h^*_{x^*x^*} \to 1/a$ as we approach the Plateau border. It follows that its length scale must be of order δL, where

$$\delta = \frac{\sqrt{h_0 a}}{L}. \tag{3.1}$$

Since $h_0 \ll L$ and a is at most $O(L)$, δ is a small parameter, representing the fact that the transition region is short compared to the lamella. Nevertheless, the slenderness parameter for the transition region,

$$\frac{h_0}{\delta L} = \frac{\epsilon}{\delta} = \sqrt{\frac{h_0}{a}},$$

is also typically small. For example, for bubbles with the following characteristic

dimensions

$$h_0 \approx 10^{-6}\,\mathrm{m}, \quad L \approx 10^{-3}\,\mathrm{m}, \quad a \approx 4 \times 10^{-4}\,\mathrm{m},$$

we find $\delta \approx 0.02$ and $\epsilon/\delta \approx 0.05$. We therefore consider the asymptotic limit $\epsilon \ll \delta \ll 1$, in which the thin-film equations may still be applied in the transition region.

Having decided on the length scale of the transition region, we obtain the appropriate velocity scaling U by balancing the first two terms in (2.3), whence

$$Ca = \frac{\epsilon}{\delta} \quad \Rightarrow \quad U = \frac{\gamma}{\mu}\sqrt{\frac{h_0}{a}}. \tag{3.2}$$

Notice that this choice of U, along with the asymptotic assumption $\epsilon \ll \delta \ll 1$ implies that capillary effects are indeed negligible in the lamella to leading order, and likewise that viscous effects are asymptotically small in the Plateau border, as hypothesized.

3.2. *Solution in the lamella*

The leading-order model in the lamella reads

$$h_t + (\bar{u}h)_x = 0, \quad (4h\bar{u}_x)_x = 0, \tag{3.3}$$

along with boundary conditions describing the symmetry of the system and the flux from the lamella into the Plateau border,

$$\bar{u} = 0 \quad \text{at} \quad x = 0, \tag{3.4}$$

$$\bar{u} = \frac{Q(t)}{h} \quad \text{at} \quad x = 1. \tag{3.5}$$

The flux Q remains to be determined by analysing the transition region. An initial condition is also required and, for simplicity, we set the thickness of the lamella to be initially uniform: $h = 1$ at $t = 0$. In this case, it is straightforward to show that h remains spatially uniform in the lamella and the solution is

$$h = h_\ell(t), \quad u = \frac{Qx}{h_\ell}, \tag{3.6}$$

where h_ℓ satisfies

$$\frac{\mathrm{d}h_\ell}{\mathrm{d}t} = -Q, \quad h_\ell(0) = 1. \tag{3.7}$$

3.3. *Solution in the transition region*

The equations in the transition region are found by scaling (2.2) and (2.3) using $x = 1 + \delta\xi$ which yields, at leading order,

$$(\bar{u}h)_\xi = 0, \tag{3.8}$$

$$(4h\bar{u}_\xi)_\xi + \tfrac{1}{2}hh_{\xi\xi\xi} = 0. \tag{3.9}$$

Boundary conditions for (3.8) and (3.9) are obtained by matching with the lamella and with the Plateau border

$$h \to h_\ell, \quad u \to h_\ell/Q \quad \text{as} \quad \xi \to -\infty, \tag{3.10}$$

$$h_{\xi\xi} \to 1 \quad \text{as} \quad \xi \to \infty, \tag{3.11}$$

Equation (3.8) implies that the flux is uniform through the transition region

$$\bar{u}h = Q(t). \tag{3.12}$$

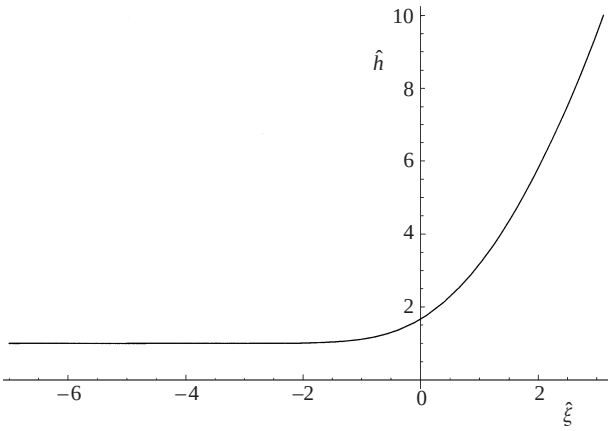

FIGURE 4. Transition region shape.

Then (3.9) becomes a quasi-steady ordinary differential equation for h, with Q as a parameter. Crucially, the boundary conditions (3.10) and (3.11) overdetermine the differential equation (3.9) and therefore give rise to a relationship between Q and h_ℓ, namely

$$Q(h_\ell) = \frac{3\sqrt{2}h_\ell^{3/2}}{16}. \tag{3.13}$$

This quantifies the Plateau border suction of liquid out of the lamella and, therefore, determines the rate at which the lamella thins. Notice that the flux is an increasing function of the lamella thickness, as might have been anticipated.

With Q given by (3.13) the transition region model may be solved analytically to give

$$2\sqrt{\hat{h}} - \frac{2}{\sqrt{3}}\arctan\left[\frac{1+2\sqrt{\hat{h}}}{\sqrt{3}}\right] + \frac{1}{3}\log\left[\frac{1-2\sqrt{\hat{h}}+\hat{h}}{1+\sqrt{\hat{h}}+\hat{h}}\right] = \sqrt{2}\hat{\xi}, \tag{3.14}$$

where $\hat{h} = h/h_\ell$, $\hat{\xi} = \xi/\sqrt{h_\ell}$ and the constant of integration (corresponding to an arbitrary translation in ξ) has been set to zero. A plot of the solution is given in figure 4; note that the profile is monotonic increasing.

Finally, we obtain the pressure in the transition region, using the scaled form of (2.5) and the solution (3.14):

$$p = -\frac{1}{2} + \frac{1}{4\hat{h}^{3/2}} + \frac{1}{4\hat{h}^3}. \tag{3.15}$$

A plot of the pressure distribution is shown in figure 5. The pressure decreases monotonically from zero in the lamella to $-\frac{1}{2}$ in the Plateau border. It is the large negative pressure in the Plateau border (compared with the lamella) that drives the flow and causes the lamella to drain.

3.4. *Lamella drainage*

The initial-value problem (3.7) satisfied by $h_\ell(t)$ is easily solved, with $Q(h_\ell)$ given by (3.13), to obtain the evolution of the lamella thickness:

$$h_\ell = \left(1 + \frac{3\sqrt{2}}{32}t\right)^{-2}. \tag{3.16}$$

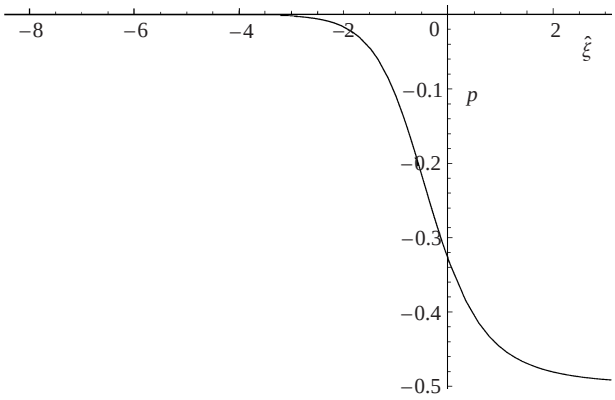

FIGURE 5. Transition region pressure profile.

The solution for h_ℓ given in (3.16) does not tend to zero in finite time. In practice, when the film becomes sufficiently thin (100 Å–1000 Å), intermolecular forces not included in this model come into play and (if destabilizing) cause the film to rupture rapidly (Erneux & Davis 1993; De Wit *et al.* 1994; Ida & Miksis 1996). The modelling of these effects involves introducing a parameter, the Hamaker constant, which is not known with any certainty. Instead, we impose a critical thickness h^*_{rup} (assumed to be a material property of the film) at which the lamella ruptures, in terms of which the dimensional lamella lifetime reads

$$t^*_{rup} = \frac{32\mu L\sqrt{a}}{3\gamma\sqrt{2}}\left[\left(\frac{1}{h^*_{rup}}\right)^{1/2} - \left(\frac{1}{h_0}\right)^{1/2}\right], \tag{3.17}$$

For water, $\mu \approx 10^{-3}\,\mathrm{kg\,m^{-1}\,s^{-1}}$ and $\gamma \approx 7\times10^{-2}\,\mathrm{N\,m^{-1}}$ and, if we suppose the film has initial thickness 1 μm and critical rupture thickness 0.1 μm, then the time to rupture is $t^*_{rup} \approx 4\times10^{-3}$ s. Clearly, for foam with a lifetime of many seconds or minutes, the presence of a surfactant must alter the dominant balance so as to slow down drainage significantly.

4. Drainage with surfactant

4.1. *Domain decomposition*

In this section, we show how ideas similar to those applied above for surfactant-free drainage may be applied to the more complicated situation where there is surfactant present. Evidently, the full equations (2.2), (2.3) and (2.6) contain several more possible physical balances than does the simplified model analysed in § 3, and it is therefore somewhat less clear how the velocity scale should be chosen. Nevertheless, it seems likely that a similar domain decomposition to that employed above should also prevail here; we anticipate that capillary effects should dominate in the Plateau border, be negligible in the lamella and balance with other physical effects in a quasi-steady transition region between the two. The length scale of the transition region is δL, as in § 3, so that it can be matched with both the lamella and the Plateau border.

Now, for velocities of practical interest ($O(10^{-3})\,\mathrm{m\,s^{-1}}$ say), the reduced capillary number Ca/ϵ is small, which implies that extensional viscous effects are negligible everywhere. This means that the theory of § 3 is not recovered by applying the limit as $Ma \to 0$ to the theory presented in this section. The intermediate regime, in which

capillary, Marangoni and extensional viscous forces all balance, does not appear to be of interest to this study, given the size of the parameters. With small capillary number we have a capillary-static Plateau border and, since the curvature of the lamella is small, we conclude that the lamella must be dominated by Marangoni forces. Our transition region in this case is therefore where the capillary and Marangoni terms balance, although we are unable to obtain a velocity scaling from such a balance, since the remaining dimensionless group in (2.3), $CaMa/\epsilon^2 = \Delta\gamma/(\epsilon^2\gamma)$, is independent of U. The surface tension gradients required to balance capillarity in (2.3), however, correspond to gradients in surfactant concentration, which must be generated by the surfactant-transport equation (2.6). Therefore, U is chosen to ensure a non-trivial balance in (2.6) in the transition region:

$$U = \frac{D}{\eta}\sqrt{\frac{h_0}{a}}. \tag{4.1}$$

As noted in Breward *et al.* (2001), surface tension gradients are ultimately set up by diffusion, and the selected velocity scale is thus diffusional.

With this choice for U, we have selected the timescale for transport by convection in the transition region, which, in terms of the parameters, reads

$$T = \frac{\delta L}{U} = \frac{\eta a}{D}. \tag{4.2}$$

Thus, for our assumption that the surfactant at the free surface is in thermodynamic equilibrium with the bulk to hold, the timescales for adsorption and adsorption must be much less than the timescale given by (4.2).

Depending on the sizes of the remaining dimensional parameters in the problem, several different asymptotic regimes may prevail. We start by considering the distinguished limit in which as many effects as possible balance in the transition region; special cases in which various terms may be neglected are considered in § 5. We therefore define

$$\mathscr{P} = \delta Pe = \frac{h_0}{\eta}, \quad \beta = \frac{\epsilon^3}{12\delta^3 Ca} = \frac{\eta\gamma h_0}{12\mu Da}, \quad \mathscr{T} = \frac{4\delta^2\Delta\gamma}{\epsilon^2\gamma} = \frac{4a\Delta\gamma}{h_0\gamma}, \tag{4.3}$$

and assume that the three parameters $\mathscr{P}$, β and $\mathscr{T}$ are all $O(1)$. Under these assumptions, we analyse separately the flows in the lamella, the Plateau border and the transition region and then match the three together. Extensional viscous forces are negligible at leading order in all three regions, so the physical structure of the problem is quite different from the pure liquid film discussed in the previous section. Here, the flow is completely governed by what is happening at the free surfaces.

4.2. *Solution in the lamella*

Under the assumptions (4.3), the flow in the lamella is extensional, diffusion is negligible and the leading-order model that holds is

$$h_t + (\bar{u}h)_x = 0, \tag{4.4}$$

$$C_x = 0, \tag{4.5}$$

$$\mathscr{P}hC_t + 2C_t + \mathscr{P}\bar{u}hC_x + 2(u_sC)_x = 0, \tag{4.6}$$

$$u_s = \bar{u}. \tag{4.7}$$

As boundary conditions, we impose symmetry at the centre of the lamella and assume a flux $Q(t)$ flows into the Plateau border,

$$u = 0 \quad \text{at} \quad x = 0, \tag{4.8}$$

$$u = \frac{Q}{h} \quad \text{at} \quad x = 1, \tag{4.9}$$

where Q remains to be determined by analysing the transition region.

Since extensional viscous effects are negligible, there is nothing to balance Marangoni stress in (4.5) and it follows that the surfactant concentration in the lamella is spatially uniform: $C = C_\ell(t)$. If a non-constant concentration were applied initially, it would rapidly equilibrate over a short time scale. Now, when the foam is initially formed, it will be wet, the bubbles spherical, and the concentration of surfactant uniform around the surface of the bubble. Since, in this paper, we are considering a dry foam, we may suppose that significant drainage has occurred and thus the concentration of surfactant contained in the lamella has decreased compared with that in the Plateau border. We model the net result of any such adjustment by imposing a uniform concentration C_I at $t = 0$, and allow $C_I \leqslant 1$ compared with $C = 1$ in the Plateau border.

We also assume, as in § 3, that the film thickness is initially uniform: $h = 1$ at $t = 0$. Then h remains spatially uniform in the lamella, and the solution of (4.4)–(4.9) is

$$h = h_\ell(t), \quad C = C_\ell(t) = C_I \frac{(2+\mathscr{P})h_\ell}{2+\mathscr{P}h_\ell}, \quad u = \frac{Q}{h_\ell}x, \tag{4.10}$$

where $h_\ell(t)$ again satisfies the initial-value problem (3.7).

4.3. *Solution in the transition region*

In the transition region, the rescaling $x = 1 + \delta\xi$ results in

$$(\bar{u}h)_\xi = 0, \tag{4.11}$$

$$hh_{\xi\xi\xi} - \mathscr{T}C_\xi = 0, \tag{4.12}$$

$$(hC_\xi)_\xi - \mathscr{P}h\bar{u}C_\xi - 2(u_sC)_\xi = 0, \tag{4.13}$$

$$u_s = \bar{u} - \tfrac{1}{2}\beta h^2 h_{\xi\xi\xi}. \tag{4.14}$$

The matching conditions with the lamella and the Plateau border read

$$h \to h_\ell, \quad \bar{u} \to \frac{Q}{h_\ell}, \quad C \to C_\ell = C_I\frac{(2+\mathscr{P})h_\ell}{2+\mathscr{P}h_\ell} \quad \text{as} \quad \xi \to -\infty, \tag{4.15}$$

$$h_{\xi\xi} \to 1, \quad C \to 1 \quad \text{as} \quad \xi \to \infty. \tag{4.16}$$

Notice our assumption here that the concentration in the Plateau border is constant; we return to this point in § 4.4.

This boundary-value problem may be simplified by solving (4.11) for $\bar{u}$, integrating (4.12) and (4.13) once each with respect to ξ and applying the matching conditions to obtain the following coupled equations for h and C:

$$\mathscr{T}(C - C_\ell) = hh_{\xi\xi} - \tfrac{1}{2}h_\xi^2, \tag{4.17}$$

$$(1 + \beta\mathscr{T}C)hC_\xi = \mathscr{P}Q(C - C_\ell) + 2Q\left(\frac{C}{h} - \frac{C_\ell}{h_\ell}\right). \tag{4.18}$$

Unfortunately, unlike the surfactant-free case, these equations cannot be solved analytically. To find the flux Q we therefore have to solve (4.17) and (4.18), with the matching conditions (4.15) and (4.16), numerically, and this is carried out for several parameter regimes of interest in § 5.

4.4. *Analysis of the Plateau border*

Here, we give a simple order-of-magnitude argument to show that the surfactant concentration is effectively constant in the Plateau border. The flux of surfactant leaving the lamella by a combination of surface and bulk convection reads, in dimensional variables,

$$\text{Flux out} \sim Q^* C_\ell^*, \tag{4.19}$$

where C_ℓ^* is the concentration in the lamella. We equate this to the flux into the Plateau border, and thus obtain, in dimensionless form,

$$\frac{\mathrm{d}C_{Pb}}{\mathrm{d}t} \sim \frac{\epsilon^3}{\delta^4} Q C_\ell. \tag{4.20}$$

Using typical parameter values, we find that $\epsilon^3/\delta^4 \approx 10^{-1}$ and conclude that, providing $Q = O(1)$ or smaller, C_{Pb} is constant on the time scale for lamella drainage.

Of course, there may well be parameter regimes in which this simple mass balance argument does imply significant variation in C_{Pb}. In a real foam, however, both the radius of curvature a and the surfactant concentration in the Plateau border are determined by the flow along the Plateau border, i.e. in the third dimension not considered here. Without addressing a much more complicated three-dimensional problem, assuming that they are both constant seems to be the most sensible option.

4.5. *Asymptotic behaviour of solutions at* $\pm\infty$

Before proceeding with the numerical solution of (4.17)–(4.18), we must check that the boundary conditions (4.15)–(4.16) are sufficient to specify the solution uniquely. To do so, we linearize about the behaviour $h \sim \frac{1}{2}\xi^2$ and $C = 1$ as $\xi \to \infty$. If Q is specified then, once translational invariance has been accounted for, the solution emanating from $\xi = +\infty$ is uniquely determined by (4.17)–(4.18) and has the asymptotic behaviour

$$h \sim \frac{\xi^2}{2} + (1 - C_\ell)\mathscr{T} + \frac{2(-\mathscr{P} + C_I(2+\mathscr{P}))Q\mathscr{T}}{3(1+\beta\mathscr{T})\xi} + O\left(\frac{1}{\xi^2}\right), \tag{4.21}$$

$$C \sim 1 + 2\frac{(-\mathscr{P} + C_I(2+\mathscr{P}))Q}{(1+\beta\mathscr{T})\xi} + O\left(\frac{1}{\xi^2}\right). \tag{4.22}$$

The qualitative behaviour of C depends on the parameter

$$\mathscr{K} = \frac{\mathscr{P}}{(2+\mathscr{P})C_I};$$

if $\mathscr{K} < 1$, then $C \to 1$ from below, otherwise, $C \to 1$ from above. Thus, we see that C does not necessarily attain its maximum value in the Plateau border.

At the other end of the range, we linearize about $h = h_\ell$, setting

$$h \sim h_\ell + a\mathrm{e}^{\lambda\xi}, \quad C \sim C_\ell + a\mathscr{T}h_\ell\lambda^2\mathrm{e}^{\lambda\xi}.$$

From (4.17) and (4.18), we obtain

$$\chi^3 - q\chi^2 + q = 0, \tag{4.23}$$

where

$$\chi = \left(\frac{h_\ell}{2} \sqrt{\frac{\mathscr{T}(2+\mathscr{P}h_\ell)}{2C_\ell}} \right) \lambda, \quad q = \frac{2Q}{h_\ell(1+\beta\mathscr{T}C_\ell)\sqrt{\mathscr{T}C_\ell}} \left(1 + \frac{\mathscr{P}h_\ell}{2}\right)^{3/2}.$$

Here, the structure of the solution depends on the sign of Q. Motivated by the purely viscous calculation of § 3, and on physical grounds, we anticipate that Q should be positive, i.e. that liquid should flow from the lamella into the Plateau border. Therefore, we assume that $q > 0$ and, because $\chi^3 - q\chi^2 + q$ has opposite signs at $\chi = 0, -1$, (4.23) has at least one negative real root, $\chi = -\chi_0(q)$ say, where

$$\chi_0 = \frac{1}{3}\left(\frac{q^2}{f(q)} + f(q) - q \right) \in (0,1), \tag{4.24}$$

and

$$f(q) = \left(\frac{27q - 2q^3 + 3\sqrt{3}q\sqrt{27-4q^2}}{2} \right)^{1/3}. \tag{4.25}$$

Note that, while $f(q) = A + \mathrm{i}B$ is complex for $q > 3\sqrt{3}/2$, χ_0, given by

$$\chi_0 = \frac{1}{3}\left(A - q + \frac{q^2 A}{A^2+B^2} + \mathrm{i}B\left(1 - \frac{q^2}{A^2+B^2}\right)\right), \tag{4.26}$$

is real, since it is easy to show by direct calculation that $A^2 + B^2 = q^2$. The other two roots are, in terms of χ_0,

$$\chi_\pm = \frac{\chi_0}{2(1-\chi_0^2)}(1 \pm \sqrt{4\chi_0^2 - 3}), \tag{4.27}$$

which are real and positive if $\chi_0 > \sqrt{3}/2$ (i.e. if $q > 3\sqrt{3}/2$) and form a conjugate pair with positive real part if $\chi_0 < \sqrt{3}/2$ (i.e. if $q < 3\sqrt{3}/2$). In terms of the original parameters, the condition for real roots is

$$\mathscr{B} = \frac{4\sqrt{2}Q(1+\mathscr{P}h_\ell/2)^2}{\sqrt{27\mathscr{X}h_\ell^3}(1+\beta\mathscr{X}h_\ell/(2+\mathscr{P}h_\ell))} < 1. \tag{4.28}$$

where $\mathscr{X} = \mathscr{T}C_I(2+\mathscr{P})$. So, as we approach $\xi = -\infty$, we find that we must suppress one growing mode (the one given by $\chi = -\chi_0$), and the other two modes decay either monotonically or in an oscillatory fashion, as dictated by the size of $\mathscr{B}$. Since Q is not known *a priori*, it is not possible to decide whether or not to expect oscillatory solutions before attempting the numerical solution. Nevertheless, if we shoot from $\xi = +\infty$ and specify h_ℓ, then there is just one free parameter Q to vary so as to eliminate the one growing mode as $\xi \to -\infty$. This suggests that the boundary-value problem (4.15)–(4.18) is indeed correctly specified and will allow us to determine the flux Q as a function of h_ℓ.

5. Numerical results

5.1. *Solution in the plug flow limit*

In this section, we present some numerical solutions of the boundary-value problem (4.15)–(4.18). We use Mathematica (see Wolfram 1999) to solve the system of equations, and we employ a shooting method from '$+\infty$': specifying h_l and varying Q until the boundary conditions at '$-\infty$' are satisfied. Initially, we consider the simplified limit

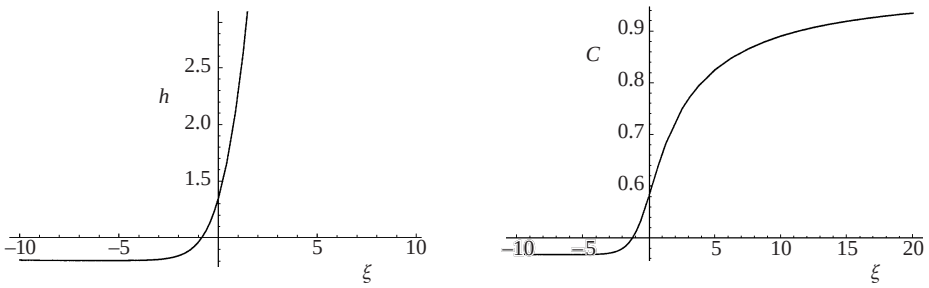

FIGURE 6. Results for thickness and concentration in a monotonic solution.

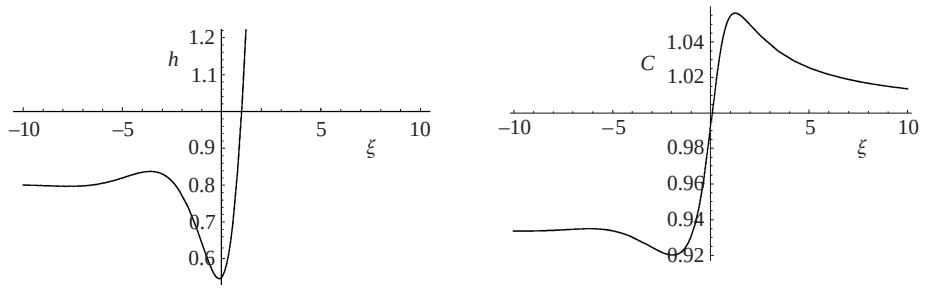

FIGURE 7. Results for thickness and concentration in a non-monotonic solution.

$\beta = 0$ so we can study how the drainage of the lamella proceeds without concerning ourselves with the parabolic flow. For each value of the lamella thickness h_ℓ, the lamella concentration C_ℓ is given by (4.10). So, once the remaining parameters $\mathscr{P}$, $\mathscr{T}$ and C_I are specified, we can in principle calculate Q for each value of h_ℓ and thus determine the rate at which the lamella drains. To demonstrate two classes of solutions to the transition region model, we start by keeping $h_\ell = 0.8$, $\mathscr{P} = 5$ and $\mathscr{T} = 5$ fixed while varying C_I.

In our first solution, we set $C_I = 0.5$ and find that $Q = 0.4292$. We calculate $\mathscr{B} = 1.405 > 1$, which implies monotonic behaviour as $\xi \to -\infty$. We also have $\mathscr{K} > 1$ and so expect $C \to 1$ from below as $\xi \to \infty$. The numerically calculated film thickness and surfactant concentrations are shown in figure 6. They exhibit monotonic increase in both h and C, as predicted.

Secondly, we set $C_I = 1$, and we find that $Q = 0.0349$. Here, we have $\mathscr{B} = 0.0808 < 1$ and $\mathscr{K} < 1$, and therefore anticipate oscillatory behaviour at $-\infty$ and that $C \to 1$ from above as $\xi \to +\infty$. Numerical plots of the film thickness and concentration of surfactant in this case are shown in figure 7. Both the film thickness and the surfactant concentration are non-monotonic in this case.

We show plots of the surface convective flux $2QC/h$, bulk convective flux $\mathscr{P}QC$ and the diffusive flux $-hC_\xi$ in figure 8(a) for the parameter values corresponding to the monotonic solution shown in figure 6. The diffusive flux is always negative, i.e. diffusion transports surfactant from the Plateau border into the lamella, while the convective fluxes are both positive, indicating that surfactant is convected from the lamella to the Plateau border. Bulk convection appears to be the dominant mechanism for surfactant transport.

We repeat this procedure for the same parameters as in the non-monotonic solution of figure 7, and plot the results in figure 8(b). Again, bulk convection and surface convection transport surfactant from the lamella into the Plateau border, but now

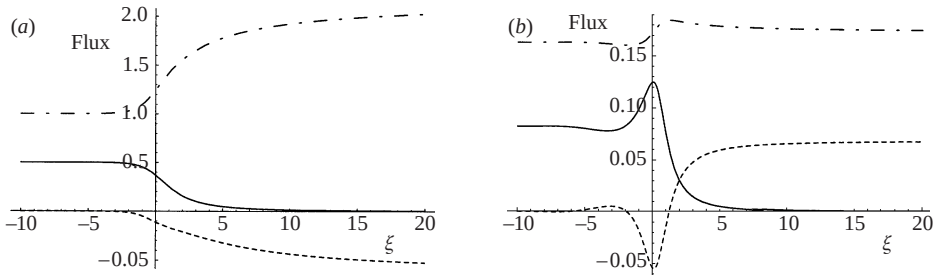

FIGURE 8. Surface convection (solid line), bulk convection (dot-dashed line) and bulk diffusion (dashed line), for (*a*) a monotonic and (*b*) a non-monotonic solution.

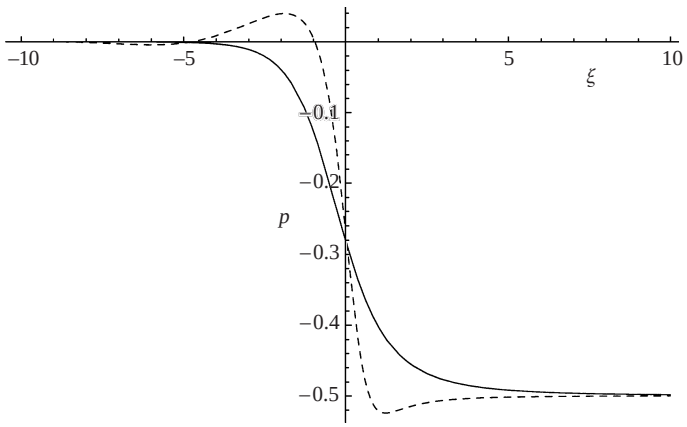

FIGURE 9. Pressure in a monotonic solution (solid) and a dimpled solution (dashed).

transport by diffusion is more complicated. Recall that the concentration profile in this parameter regime is non-nomotonic, and that the concentration achieves a maximum within the transition region. As might be anticipated, diffusion transports surfactant out from this maximum (both towards the Plateau border and further into the transition region).

We now calculate the pressure in the transition region using

$$p = -\tfrac{1}{2}h_{\xi\xi} \tag{5.1}$$

(recall that the extensional viscous term is negligible here). Unsurprisingly, in a monotonic solution, shown as a solid curve in figure 9, the pressure decreases monotonically from 0 to $-\frac{1}{2}$, whereas in a non-monotonic solution, shown as a dashed curve, the pressure variation is likewise non-monotonic. In the latter case, the pressure attains a positive maximum in the transition region before a sudden decrease and then tends to $-\frac{1}{2}$ from below, behaviour similar to that dismissed by Barigou & Davidson (1994). They impose a sharp change in boundary structure (from a stress-free boundary in the lamella to a no-slip boundary in the transition region), which gives rise to a step increase in pressure at the inlet to the contraction zone. It is this step that they reject as unphysical. Our model describes a gradual change in stress at the surface, and we obtain a smooth profile for the pressure in a non-monotonic solution. We therefore see no reason to reject this type of solution on the basis of the pressure profile.

We now generate $Q = Q(h_\ell)$ for a given set of parameters, setting $\mathscr{P} = 0.5$, $\mathscr{T} = 0.5$, $C_I = 0.1$, and varying h_ℓ from 0.1 to 1. The variation of Q with h_ℓ is shown in figure 10.

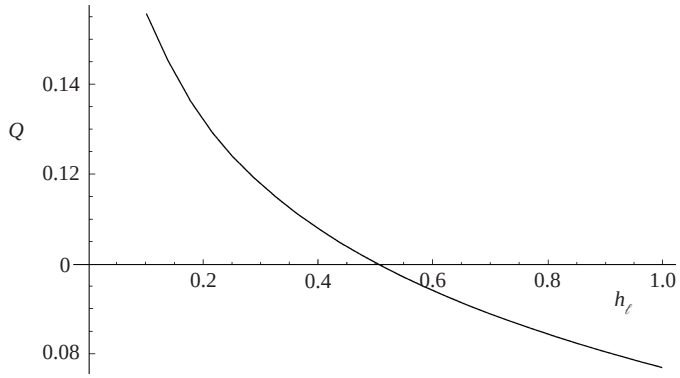

FIGURE 10. Graph showing Q as a function of h_ℓ for $\mathscr{P} = 0.5$, $\mathscr{T} = 0.5$ and $C_I = 0.1$.

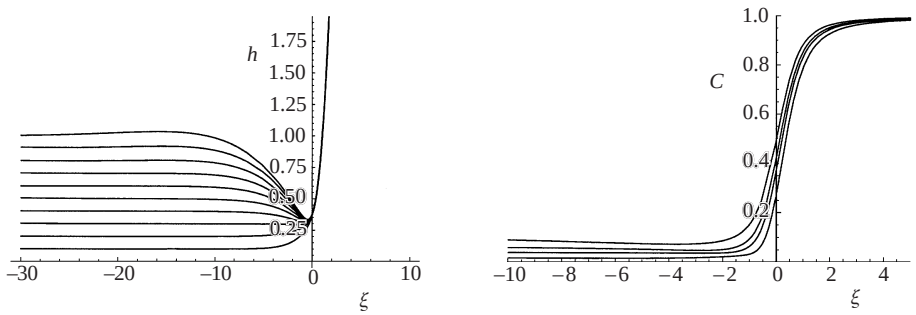

FIGURE 11. Transition region thickness and concentration for various values of h_ℓ, with $\mathscr{P} = 0.5$, $\mathscr{T} = 0.5$ and $C_I = 0.1$.

Surprisingly, the flux increases as h_ℓ decreases, in contrast with the surfactant-free case. We return to examine this behaviour further in § 6.

We show the thickness of the transition region and the corresponding concentration profiles for h_ℓ between 0.1 and 1 (using the same parameter values) in figure 11. These may be thought of as time snapshots of the transition region as the lamella thins from $h_\ell = 1$ to $h_\ell = 0.1$. We calculate $\mathscr{B}$ for each of the snapshots and find that, for $h_\ell \geqslant 0.6$, $\mathscr{B} < 1$, while for the other solutions $\mathscr{B} > 1$. Examining the solutions closely for large negative ξ, we see that the solutions are indeed oscillatory when $h_\ell \geqslant 0.6$. Notice that the condition (4.28) for oscillatory solutions contains the factor $Q/h_\ell^{3/2}$, which increases as h_ℓ decreases, with the flux as shown in figure 10. Hence, (4.28) implies that the oscillations at $-\infty$ die away as the film thins, as is supported by the numerical evidence. Note, however, that for $h_0 = 0.3$, 0.4 and 0.5, a single dimple remains close to $\xi = 0$ even after the small oscillations have died away. This nonlinear effect results from the interplay between all the physical mechanisms included in the model, and there does not seem to be any simple physical or mathematical criterion for the appearance of this phenomenon. However, we note that dimples were seen in the experiments described in Joye *et al.* (1992).

We are now in a position to determine the time taken for the lamella to drain. With $Q(h_\ell)$ as shown in figure 10, we integrate (3.7) numerically to find the evolution of the lamella thickness, as shown in figure 12. From the graph, it appears that h_ℓ may tend to zero in finite time. Whether this does occur depends on the behaviour of Q as $h_\ell \to 0$. It is difficult to obtain this behaviour accurately from the numerical

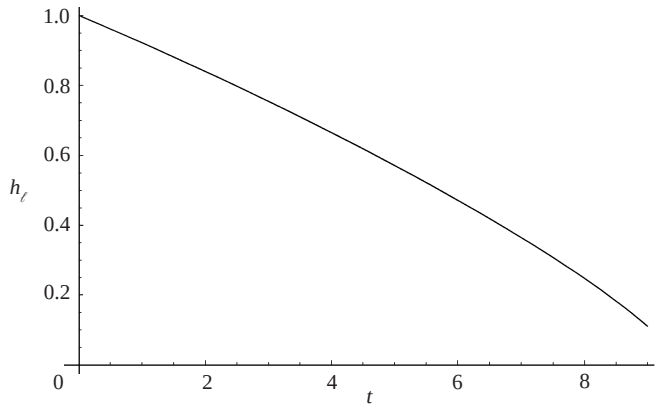

FIGURE 12. Graph showing lamella thickness versus time for $\mathscr{P} = 0.5$, $\mathscr{T} = 0.5$ and $C_I = 0.1$.

solution of (4.15)–(4.18), and in fact there is a serious problem with the limit $h_\ell \to 0$, as we shall see in § 6. In any case, as pointed out in § 3.1, when the lamella becomes sufficiently thin, other physical effects not included here become important. As there, we impose a critical thickness $h^*_{rup} = 0.1\, h_0$ at which the lamella ruptures. The lifetime of the lamella is then the time taken for h_ℓ to decrease from 1 to 0.1, which we calculate to be $t_{rup} = 9.085$.

Using the time scale $L/U \approx 10\,\mathrm{s}$, we calculate the dimensional rupture time to be $t^*_{rup} \approx 90\,\mathrm{s}$ for the parameter values chosen here. This is of the correct order and is certainly much closer to the time scale for rupture of a typical foam film than the prediction given by the surfactant-free theory.

5.2. *Solution with parabolic flow*

We now reintroduce the parabolic velocity profile, i.e. allow β to be non-zero, and examine the flow behaviour as we approach the Plateau border. Using (2.4) and the asymptotic form for h given in (4.21), we find expressions for the surface velocity u_s and the centreline velocity u_{cl}, given by

$$u_s = \tfrac{1}{2}[(2+\mathscr{P})C_I - \mathscr{P}]\beta Q\mathscr{T} + O\left(\frac{1}{\xi}\right), \tag{5.2}$$

$$u_{cl} = -\tfrac{1}{4}[(2+\mathscr{P})C_I - \mathscr{P}]\beta Q\mathscr{T} + O\left(\frac{1}{\xi}\right). \tag{5.3}$$

Thus, $u_s > 0$, $u_{cl} < 0$ if $\mathscr{K} < 1$ and vice versa. Since u_s and u_{cl} always take different signs, eddies are set up at the entrance to the Plateau border, with direction of rotation being determined by $\mathscr{K}$.

We solve the transition region model and, again, observe both monotonic and nonmonotonic solutions. Now that the liquid velocity is no longer uniform, we visualize the flow by plotting the velocity field, using the vertical component

$$v = \frac{Q}{h^2}h_x y - \beta h_{xxxx}\left(\frac{h^2}{4}y - y^3\right) - \frac{\beta}{2}hh_x h_{xxx}y. \tag{5.4}$$

First, we illustrate a monotonic solution by setting $\mathscr{T} = 5$, $\mathscr{P} = 5$, $C_I = 0.5$, $h_\ell = 0.8$ and $\beta = 1$, for which we find that $Q = 2.008$ and hence $\mathscr{B} = 1.97 > 1$. Since $\mathscr{K} > 1$, we predict $u_s < 0$, $u_{cl} > 0$ as $\xi \to \infty$. We show the transition region shape and the velocity field in figure 13. We observe a monotonic profile, in which

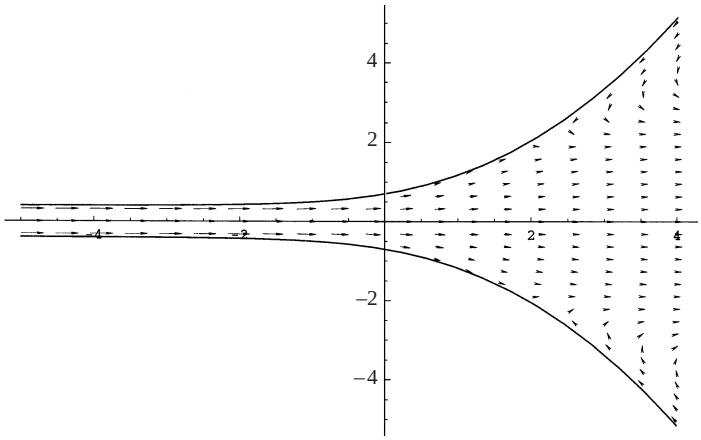

FIGURE 13. Velocity field for a solution where $\mathscr{K} > 1$.

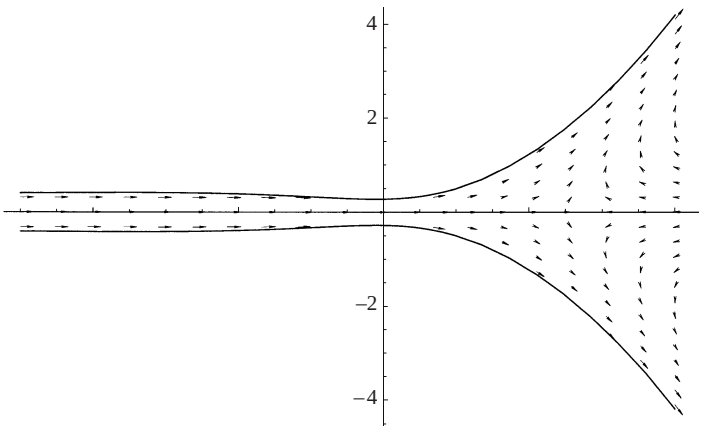

FIGURE 14. Velocity field for a solution where $\mathscr{K} < 1$.

the velocity decreases as the liquid approaches the Plateau border, and the centreline velocity remains positive while the surface velocity becomes negative. Eddies are set up at the entrance to the Plateau border which remove liquid from the border along the free surfaces and return liquid to the border along the centreline.

As a second example, we set $\mathscr{T} = 5$, $\mathscr{P} = 5$, $C_I = 1$, $h_\ell = 0.8$ and $\beta = 1$, and find $Q = 0.2095$. We calculate $\mathscr{B} = 0.086 < 1$, implying oscillatory behaviour at $-\infty$, and since $\mathscr{K} < 1$, we expect that $u_s > 0$ and $u_{cl} < 0$ as $\xi \to +\infty$. Plots of the transition region shape and velocity field in this case are shown in figure 14. We observe a non-monotonic solution in which the velocity decreases in magnitude as the liquid approaches the Plateau border, this time becoming negative on the centreline while remaining positive on the free surfaces. In contrast to the previous case, eddies are now set up at the entrance to the Plateau border which remove liquid from the border along the centreline and return liquid to the border along the free surfaces.

It is worth emphasizing that the cases $u_s > 0$ and $u_s < 0$ are not dependent on whether the solution is monotonic, but merely on whether $\mathscr{K}$ is greater or less than 1 (which also determines whether C approaches 1 from below or above). To illustrate this, we show the surface and centreline velocities as β is increased from zero to one for each of these two cases in figure 15.

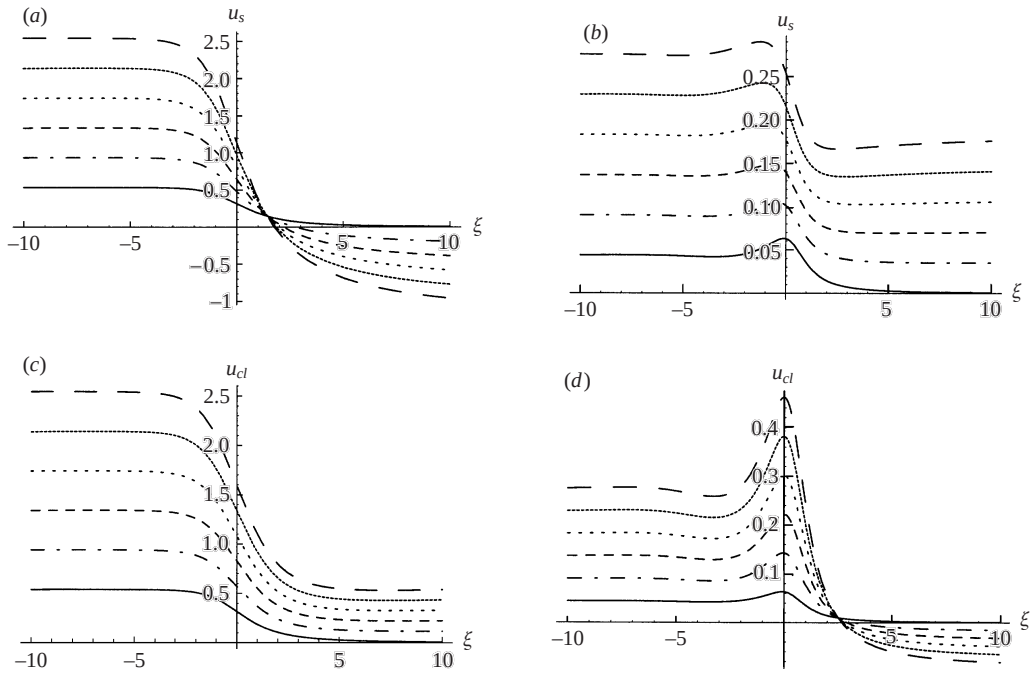

FIGURE 15. Graphs showing surface velocity u_s and centreline velocity u_{cl} for the cases $\mathscr{K} > 1$ ((*a*) and (*c*)) and $\mathscr{K} < 1$ ((*b*) and (*d*)), with $\beta = 0$ (solid line), 0.2 (dot-dashed line), 0.4 (small-dashed line), 0.6 (wide-spaced dotted line), 0.8 (close-spaced dotted line) and 1.0 (large-dashed line).

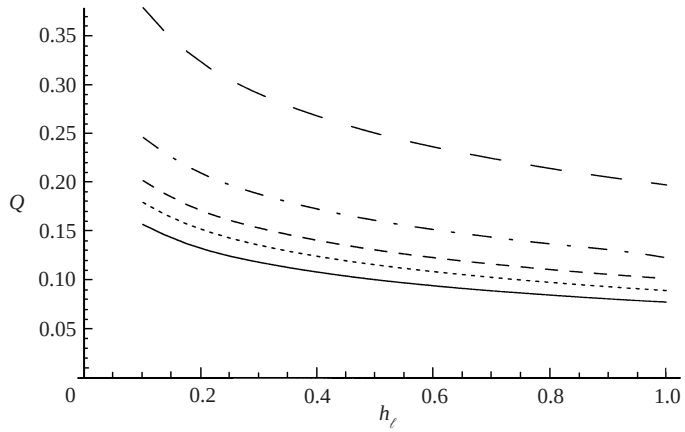

FIGURE 16. Graph showing how the flux varies with h_ℓ, for $\beta = 0$ (solid line), 0.5 (dotted line), 1 (small-dashed line), 2 (dot-dashed line) and 5 (large-dashed line). The other parameters are taken to be $\mathscr{P} = 0.5$, $\mathscr{T} = 0.5$ and $C_I = 0.1$.

When $\beta = 0$, the liquid velocity is everywhere positive. With $\mathscr{T} = 5$, $\mathscr{P} = 5$ and $C_I = 0.5$ so that $\mathscr{K} > 1$, increasing β from zero (with C_I and $\mathscr{P}$ fixed) creates a stagnation point which travels down the free surface from $\xi = +\infty$. The centreline velocity remains positive everywhere in this case. With $\mathscr{T} = 5$, $\mathscr{P} = 5$ and $C_I = 1$ so that $\mathscr{K} < 1$, increasing β from zero creates a stagnation point on the centreline which travels in from infinity, while the surface velocity remains positive.

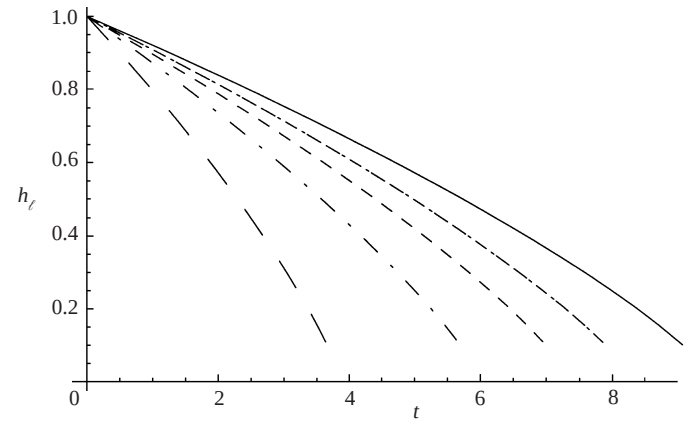

FIGURE 17. Graph showing how the thickness of the lamella varies with time, for $\beta = 0$ (solid line), 0.5 (dotted line), 1 (small-dashed line), 2 (dot-dashed line) and 5 (large-dashed line). The other parameters are taken to be $\mathscr{P} = 0.5$, $\mathscr{T} = 0.5$ and $C_I = 0.1$.

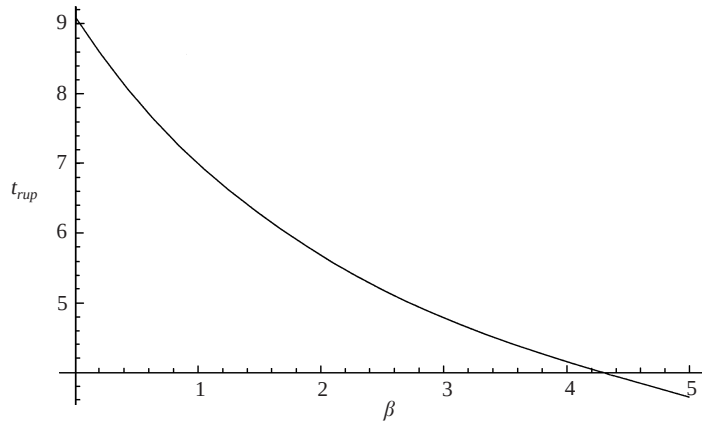

FIGURE 18. Graph showing how the rupture time varies with β. The other parameters are taken to be $\mathscr{P} = 0.5$, $\mathscr{T} = 0.5$ and $C_I = 0.1$.

Finally, we fix a given set of parameters, $\mathscr{P} = 0.5$, $\mathscr{T} = 0.5$ and $C_I = 0.1$, vary h_ℓ between 0.1 and 1, and calculate $Q(h_\ell)$, for various values of β, as shown in figure 16. As for $\beta = 0$, we find that Q increases as h_ℓ decreases. We also see that the flux increases as β increases. By integrating (3.7), we then determine the evolution of the lamella thickness h_ℓ, as shown in figure 17, and thereby estimate the rupture time as the time for h_ℓ to decrease to a tenth of its original value as a finction of β, as shown in figure 18. We see that the time to rupture decreases as β increases. For $\beta = 1$, we find that the rupture time is $t_{rup} = 6.99$, and thus the dimensional lamella lifetime is $t^*_{rup} \approx 70\,\mathrm{s}$, which is slightly smaller than the corresponding value with $\beta = 0$. We stress that the main effect of including non-zero β is that it either retards the surface flow and accelerates the centreline flow, or vice versa, depending on the size of $\mathscr{K}$. It appears that its net effect on the drainage rate is relatively small.

5.3. *Solution with negligible diffusion*

In this section, we consider the parameters relevant to a solution of the surfactant CTAB (described in detail in Manning-Benson *et al.* 1997; Bain *et al.* 2000), which has

diffusivity $D \approx 5 \times 10^{-10}\,\mathrm{m^2\,s^{-1}}$ and adsorption length $\eta \approx 10^{-5}\,\mathrm{m}$. The viscosity and surface tension are given by $\mu \approx 10^{-3}\,\mathrm{kg\,m^{-1}\,s^{-1}}$ and $\gamma \approx 7 \times 10^{-2}\,\mathrm{N\,m^{-1}}$, while the variation of surface tension with concentration is $(\mathrm{d}\gamma^*/\mathrm{d}C^*) \approx 2.5 \times 10^{-2}\,\mathrm{N\,m^2\,mol^{-1}}$. We consider a dilute solution with $C_0 \approx 2 \times 10^{-3}\,\mathrm{mol\,m^{-3}}$, and a lamella with the same approximate dimensions as in § 3, namely $h_0 \approx 10^{-6}\,\mathrm{m}$, $L \approx 10^{-3}\,\mathrm{m}$, $a \approx 4 \times 10^{-4}\,\mathrm{m}$. The relevant dimensionless parameters are found to be

$$\mathscr{P} \approx 10^{-1}, \quad \beta \approx 300, \quad \mathscr{T} \approx 1.$$

The size of β indicates that the velocity scaling chosen in (4.1) is inappropriate here; u should be rescaled with β, which corresponds to choosing

$$U = \frac{\gamma}{12\mu}\left(\frac{h_0}{a}\right)^{3/2} \approx 7 \times 10^{-4}\,\mathrm{m\,s^{-1}}. \tag{5.5}$$

Note that this is an order of magnitude smaller than the pure viscous velocity scale (3.2). Our time scale for lamella drainage then becomes $T = L/U = 1.4\,\mathrm{s}$, while the time scale for convection in the transition region becomes $T = L\delta/U = 3 \times 10^{-2}\,\mathrm{s}$. Thus, in order for our assumption of thermodynamic equilibrium to be valid, the time scales for adsorption and desorption must be much less than $3 \times 10^{-2}\,\mathrm{s}$.

The domain decomposition performed in § 4 also applies here; we have a capillary-static Plateau border, in which the surfactant concentration is effectively constant, and a Marangoni-dominated lamella, in which exactly the same model (4.4)–(4.9) applies. The only difference comes when we consider the transition region, where we find that the new velocity scale makes diffusion $O(1/\beta)$ compared to convection. If we therefore neglect diffusion, the transition region model becomes

$$(\bar{u}h)_\xi = 0, \tag{5.6}$$

$$hh_{\xi\xi\xi} - \mathscr{T}C_\xi = 0, \tag{5.7}$$

$$\mathscr{P}^* h\bar{u}C_\xi + 2(u_s C)_\xi = 0, \tag{5.8}$$

$$u_s = \bar{u} - \tfrac{1}{2}h^2 h_{\xi\xi\xi}, \tag{5.9}$$

with the same matching conditions as before. Here, $\mathscr{P}^* = h_0/\eta$.

Now, it might have been anticipated that neglecting diffusion would lead to a reduction of order and hence a singular perturbation problem. This does not occur because, as in Breward *et al.* (2001), the fluid–surfactant interaction gives rise to a diffusive term quite independently of any bulk or surface diffusion. This can be seen from the simplification of (5.6)–(5.9) analogous to (4.17)–(4.18), namely

$$\mathscr{T}(C - C_\ell) = hh_{\xi\xi} - \tfrac{1}{2}h_\xi^2, \tag{5.10}$$

$$\mathscr{T}hCC_\xi = \mathscr{P}Q(C - C_\ell) + 2Q\left(\frac{C}{h} - \frac{C_\ell}{h_\ell}\right). \tag{5.11}$$

This diffusion-free model is likely to apply to many different surfactants whose diffusion coefficient is similar to that for CTAB.

Guided by the parameter values estimated above, we set $\mathscr{T} = 1$, $\mathscr{P}^* = 0.1$ and $C_I = 0.1$. As before, we vary h_ℓ between 0.1 and 1 to find Q as a function of h_ℓ. We show the solution for Q as a function of h_ℓ in figure 19; the behaviour is qualitatively the same as that shown in figure 10. In this case, the dimensional rupture time is found to be $t^*_{rup} \approx 5\,\mathrm{s}$, which is a plausible time scale for the collapse of a film stabilized by

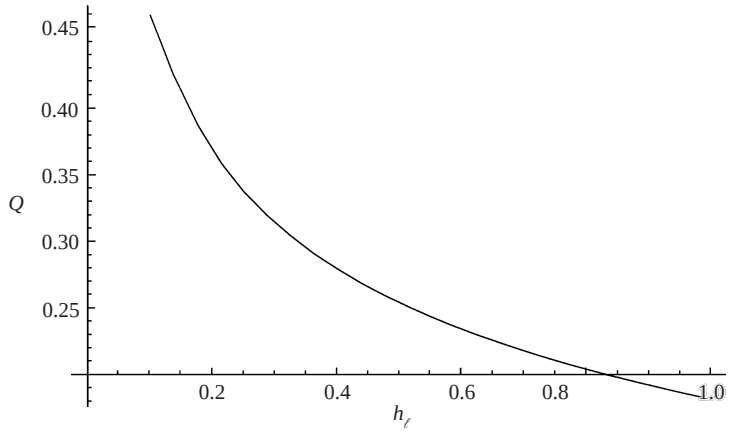

FIGURE 19. Graph showing Q against h_ℓ for $\mathscr{P}^* = 0.1$, $\mathscr{T} = 1$ and $C_I = 0.1$.

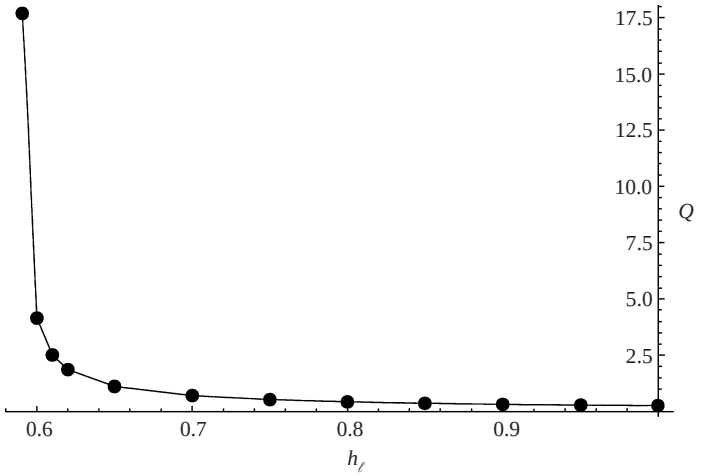

FIGURE 20. Graph showing Q against h_ℓ for $C_I = 0.5$, $\mathscr{P} = 5$ and $\mathscr{T} = 5$.

CTAB. Neglecting diffusion has not made an appreciable difference to the qualitative behaviour of the model.

6. The large-flux limit

While attempting to find numerical solutions to the transition region model, we observed the following unexpected behaviour. For certain parameter regimes, Q appears to approach infinity at a finite value of h_ℓ. We illustrate this behaviour in figure 20, for the regime $C_I = 0.5$, $\mathscr{P} = 5$, $\beta = 0$ and $\mathscr{T} = 5$. We were unable to find a value of Q for $h_\ell \leqslant 0.59$ in this case. In this section, we present an asymptotic argument as to why this occurs, which also explains why the flux increases as the thickness decreases in the solutions presented earlier.

It is convenient to eliminate C between (4.17) and (4.18), and then to reduce the order by setting $h_\xi^2 = g(h)$ (the solutions of interest here are all monotonic, so there

is no difficulty in defining $g(h)$). The problem becomes

$$(1+\beta\mathscr{T}C_\ell+\tfrac{1}{2}\beta(hg_h-g))\sqrt{g}g_{hh}=\frac{Q}{h^3}(2+\mathscr{P}h)(hg_h-g)+\frac{4Q\mathscr{T}C_\ell}{h^3}\left(1-\frac{h}{h_\ell}\right), \quad (6.1)$$

where

$$g(h_\ell)=0, \quad g'(h_\ell)=0, \quad (6.2)$$

$$g\sim 2h-2\mathscr{T}(1-C_\ell) \quad \text{as} \quad h\to\infty. \quad (6.3)$$

Now, instead of seeking Q as a function of h_ℓ, we let $Q\to\infty$ and deduce the corresponding behaviour of h_ℓ.

Note that the limit $Q\to\infty$ is singular since it removes the highest derivative in (6.1). However, as h becomes large to match with the Plateau border, this term comes back in at leading order. The appropriate scaling depends on β. If $\beta=0$, we choose $h=Q^2H$ and $g=Q^2G$, after which we seek an outer solution as an asymptotic expansion in powers of $1/Q^2$.

The leading-order problem reads

$$H^3\sqrt{G_0}G_{0HH}=\tfrac{1}{2}\mathscr{P}H(HG_{0H}-G_0), \quad (6.4)$$

with

$$G_0\sim 2H \quad \text{as} \quad H\to\infty. \quad (6.5)$$

It is fortunate that we can spot a solution to (6.4) that also satisfies (6.5), namely

$$G_0=2H. \quad (6.6)$$

We need not look for a more general solution since we have already established that the solution emanating from $\xi=\infty$ is unique.

If $\beta\neq 0$, the appropriate scaling is $h=Q^{2/3}H$ and $g=Q^{2/3}G$, after which we seek an asymptotic expansion in powers of $1/Q^{2/3}$. The leading-order problem in this case reads

$$\tfrac{1}{2}\beta(HG_{0H}-G_0)H^3\sqrt{G_0}G_{0HH}=\mathscr{P}(HG_{0H}-G_0), \quad (6.7)$$

with (6.5). As in the $\beta=0$ case, the unique solution is (6.6).

We now consider (6.1) in the limit $Q\to\infty$. We seek an asymptotic solution in powers of $1/Q$, and find that the leading-order solution which matches with (6.6) reads

$$g_0=2h\left[1+\frac{C_I(2+\mathscr{P})\mathscr{T}}{2}\log\left(\frac{\mathscr{P}h}{2+\mathscr{P}h}\right)\right]+\frac{2\mathscr{T}C_I(2+\mathscr{P})h_\ell}{2+\mathscr{P}h_\ell}. \quad (6.8)$$

Now we find h_ℓ as a function of Q (in the limit $Q\to\infty$) by applying the left-hand boundary conditions $g(h_\ell)=g'(h_\ell)=0$. We set

$$h_\ell\sim h_c+h_{c1}/Q+h_{c2}/Q^2+\cdots,$$

so that h_c is the value of h_ℓ (if it exists) at which Q approaches infinity, and satisfies $g_0(h_c)=0$, i.e.

$$2h_c\left[1+\frac{C_I\mathscr{T}(2+\mathscr{P})}{2}\log\left(\frac{\mathscr{P}h_c}{2+\mathscr{P}h_c}\right)\right]+\frac{2\mathscr{T}C_I(2+\mathscr{P})h_c}{2+\mathscr{P}h_c}=0. \quad (6.9)$$

For given C_I, $\mathscr{P}$ and $\mathscr{T}$, (6.9) has one positive solution h_c satisfying $g_0(h_c)=g_0'(h_c)=0$; the trivial solution $h_c=0$ can be rejected since $g_0'(0)\neq 0$.

For $\mathscr{T}=5$, $\mathscr{P}=5$ and $C_I=0.5$, the solution is $h_c\approx 0.587$, so our numerical

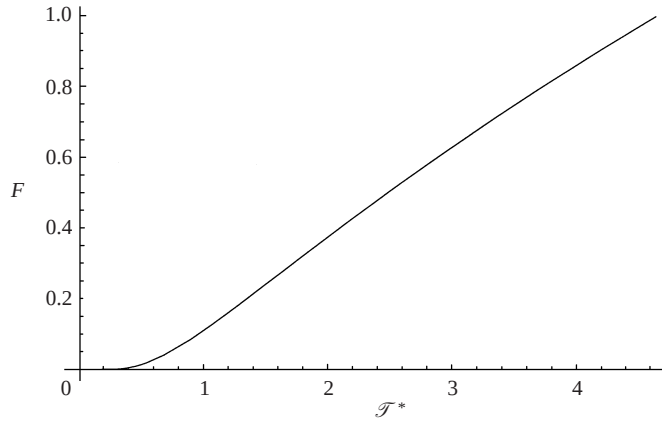

FIGURE 21. Graph showing the function $F(\mathscr{T}^*)$ defined in (6.11).

observation that $Q \to \infty$ for h_ℓ close to 0.59 can be explained asymptotically. Two questions remain: first, why did we not observe similar behaviour in our other numerical calculations; and secondly, what happens after h_ℓ reaches h_c?

With $\mathscr{T} = 0.5$, $\mathscr{P} = 0.5$ and $C_I = 0.1$, we calculate $h_c = 4.4 \times 10^{-7}$. Thus, for these particular parameter values, Q tends to infinity at a value of h_ℓ that is practically zero, in agreement with the behaviour plotted in figure 10 from our numerical calculations. In general, the positive solution of (6.9) can be written as

$$h_c = \frac{1}{\mathscr{P}} F(\mathscr{T}^*) \quad \text{where} \quad \mathscr{T}^* = C_I(2+\mathscr{P})\mathscr{T}, \tag{6.10}$$

and the function F is given inplicitly by

$$\mathscr{T}^* = -\frac{2(2+F(\mathscr{T}^*))}{(2+F(\mathscr{T}^*))\log\left[\dfrac{2+F(\mathscr{T}^*)}{F(\mathscr{T}^*)}\right]+2}. \tag{6.11}$$

The behaviour of $F(\mathscr{T}^*)$ is shown in figure 21. Notice that $F(\mathscr{T}^*)$ has asymptotic behaviour

$$F \sim 2\exp\left(-1-\frac{2}{\mathscr{T}^*}\right) \quad \text{as} \quad \mathscr{T}^* \to 0 \tag{6.12}$$

and hence, if $\mathscr{T}^*$ is small, then F is exponentially small. This explains why, for many of our calculations, h_c was effectively zero (to within our numerical tolerance) and we did not observe Q tending to infinity at finite h_ℓ.

At the other extreme, $F \sim \sqrt{\mathscr{T}^*}$ as $\mathscr{T}^* \to \infty$ and so, for large enough $\mathscr{T}^*$, we will have $h_c > 1$. This corresponds to the critical thickness exceeding the initial thickness of the lamella, and in such a case we cannot even start to follow the evolution of h.

In practice, the flux cannot become infinite on physical grounds. As Q becomes large, some physical effects that have been neglected, for example the extensional viscous term in (2.3) or inertia, must become important and regularize the model. Moreover, the inclusion of these effects should then allow the behaviour of Q for $h < h_c$ to be described, and we plan to pursue this approach in future work (see § 7). For the moment, we hypothesize that the result of such an analysis would be that the lamella rapidly thins and ruptures, over a time scale much shorter than that considered here, once the lamella thickness reaches its critical value.

7. Conclusions and discussion

In this paper, we have developed and analysed models describing surfactant-free and surfactant-stabilized drainage of a foam lamella. Our solution procedure involves decomposing the liquid domain into a capillary-static Plateau border, a time-dependent thinning film and a quasi-steady transition region between the two. In the absence of surfactant, the lamella is governed by viscous effects, the Plateau border by capillary effects and the transition region by a combination of the two. By drawing on the solution of an analogous problem by Howell (1999), we obtained the flux $Q(h_\ell)$ of liquid from the lamella into the Plateau border as a function of the lamella thickness h_ℓ. The flux decreases as the lamella thickness decreases, such that it takes an infinite time for the thickness to reach zero. We therefore imposed a critical thickness at which the lamella spontaneously ruptures to estimate the lamella lifetime. For typical parameter values, this lifetime is extremely short without the stabilizing influence of surfactant.

In the presence of a soluble surfactant, we performed a similar domain decomposition, this time into a Marangoni-dominated lamella, a capillary-static Plateau border and a transition region in which Marangoni and capillary forces balance. We found an explicit relationship (4.10) between the surfactant concentration and the film thickness in the lamella. We also obtained a coupled boundary-value problem, (4.15)–(4.18), for the concentration and film thickness in the transition region. This problem must, in general, be solved numerically, but we showed that it is sufficient, in principle, to determine the flux Q of liquid from the lamella into the Plateau border as a function of the lamella thickness h_ℓ.

We performed numerical calculations to illustrate several classes of solution that may arise for three particular parameter regimes of interest. In the first case, there is a plug flow in the transition region and the film thickness may or may not be monotonic. It is interesting that lamellae with dimpled edges have been reported experimentally, and our model may provide a mechanism for such observations. We found that the flux increases as the film thickness decreases, in contrast with the surfactant-free case, which suggests the possibility of finite-time rupture. Using typical parameter values, we estimated a time to rupture of the order of 10^2 s, which indicates that surfactant effects can indeed greatly enhance lamella lifetime.

In the second case considered, the transition region flow is parabolic. We showed that eddies are produced at the entrance to the Plateau border, which may either draw liquid into the Plateau border along the centreline and out along the free surfaces or vice versa. The latter behaviour is counter-intuitive, since we expect Marangoni traction at the free surfaces to oppose Plateau border suction. We determined the condition on the physical parameters that distinguishes between these two possibilities. Non-uniformity of the flow in the transition region was found to have a relatively small effect on the drainage rate, and hence on the lamella lifetime, compared with the plug flow case.

Using parameters for a typical surfactant, we showed that transport by diffusion may be neglegible. We found that ignoring diffusion does not reduce the order of the problem, because of the diffusive nature of the fluid–surfactant interaction. Realistic parameters for a dilute surfactant solution give a rupture time scale of order 10 s.

In all these situations, the introduction of surfactant increases the time scale for lamella rupture and results in a flux that increases as the lamella thickness decreases. Physically, since the viscous stress due to the liquid flow is negligible, the dominant stress balance is between the Marangoni traction and the capillary pressure. The flux alters so as to provide the distribution of surface surfactant that is required to generate the Marangoni traction.

In some parameter regimes, we found that the flux appears numerically to approach infinity at a finite critical value h_c of the lamella thickness. We showed that this behaviour is, in fact, generic, although h_c may be extremely small in many cases. Physically, when the film is thick, the dominant mechanism for surfactant transport is bulk convection, which tends to sweep surfactant towards the Plateau border. As the film thins, surface convection becomes increasingly important. When these two effects balance, an infinite flux is required to cause the order one change in the concentration of surfactant that is necessary to provide the appropriate level of Marangoni traction.

We plan to examine the issue of the critical thickness in a subsequent study that includes further physical effects when the flux becomes large, and thus allows us to continue our solution below $h = h_c$. Candidate mechanisms include extensional viscous effects, inertia and surface viscosity. We intend to investigate the ability of each of these to regularize the problem and thus allow us to describe fully the drainage of a lamella from its initial thickness to its rupture thickness

We have, throughout this paper, assumed that the surfactant concentration is small. To relax this approximation, we would have to use nonlinear relationships between the bulk and surface concentrations and the surface tension (the Langmuir isotherm and the Frumkin equation, respectively; see Adamson 1982), resulting in a more complicated system. Nevertheless, the solution procedure would be identical to that described in this paper and we would expect the results to be qualitatively similar. Note that the inclusion of a nonlinear relationship between the surface tension and surface concentration of surfactant can result in the localization of surfactant in some situations (see Naire, Braun & Snow 2001).

The analysis of our mathematical model illuminates the well-documented phenomenon that differences in the surface concentration of surfactant between a lamella and a Plateau border in a foam drive a flow of liquid which retards the inherent liquid drainage into the Plateau border. Stagnation points may develop on the free surface and a parabolic flow profile can develop in the 'entrance' to the Plateau border (i.e. in our transition region). These observations are often presented using arguments that are less precise (Barigou & Davidson 1994, for example) than those given in this paper.

Our long-term goal is to use the insight into lamella drainage that we have gained here as a building block in the generation of a macroscopic model to describe foam behaviour.

The authors are very grateful for the assistance and advice of Professor R. C. Darton and Dr J. R. Ockendon, and for many helpful discussions with Dr S. D. Howison and Dr C. D. Bain. Part of this work was carried out with the financial support of an EPSRC studentship (C. J. W. B.) and a Junior Research Fellowship from Christ Church, Oxford (P. D. H.).

REFERENCES

Adamson, A. W. 1982 *Physical Chemistry of Surfaces*, 4th edn. J. Wiley.

Atkins, P. W. 1999 *Physical Chemistry*, 6th edn. Oxford University Press.

Bain, C. D., Manning-Benson, S. & Darton, R. C. 2000 Rates of mass transfer and adsorption of CTAB at an expanding air–water interface. *J. Colloid Interface Sci.* **229**, 247–256.

Barigou, M. & Davidson, J. F. 1994 Soap film drainage: theory and experiment. *Chem. Engng Sci.* **49**, 1807–1819.

Braun, R., Snow, S. A. & Pernisz, U. C. 1999 Gravitational drainage of a tangentially-immobile thick film. *J. Colloid Interface Sci.* **219**, 225–240.

Breward, C. J. W. 1999 The mathematics of foam. DPhil. thesis, Oxford University.

Breward, C. J. W., Darton, R. C., Howell, P. D. & Ockendon, J. R. 1997 Modelling foam drainage. *IChemE Symp Series* **142**, 1009–1019.

Breward, C. J. W., Darton, R. C., Howell, P. D. & Ockendon, J. R. 2001 The effect of surfactants on expanding free surfaces. *Chem. Engng Sci.* **56**, 2867–2878.

Chang, C. H. & Franses, E. I. 1995 Adsorption dynamics of surfactants at the air–water interface: a critical review of mathematical models and mechanisms. *Colloids Surfaces* A: *Physicochem. Engng Aspects* **100**, 1–45.

De Wit, A., Gallez, D. & Christov, C. I. 1994 Nonlinear evolution equations for thin liquid films with insoluble surfactants. *Phys. Fluids* **6**, 3256–3265.

Erneux, T. & Davis, S. H. 1993 Nonlinear rupture of free films. *Phys. Fluids* A **5**, 1117–1122.

Howell, P. D. 1996 Models for thin viscous sheets. *Eur. J. Appl. Maths* **7**, 321–343.

Howell, P. D. 1999 The draining of a two-dimensional bubble. *J. Engng Maths* **35**, 251–272.

Howell, P. D. & Breward, C. J. W. 2002 Mathematical modelling of the overflowing cylinder experiment. *J. Fluid Mech.* (submitted).

Ida, M. P. & Miksis, M. J. 1996 Thin film rupture. *Appl. Maths Lett.* **9**, 35–40.

Ida, M. P. & Miksis, M. J. 1998*a* The dynamics of thin films I: general theory. *SIAM J. Appl. Maths* **58**, 456–473.

Ida, M. P. & Miksis, M. J. 1998*b* The dynamics of thin films II: applications. *SIAM J. Appl. Maths* **58**, 473–500.

Joye, J. L., Miller, C. A. & Hirasaki, G. J. 1992 Dimple formation and behavior during axisymmetrical foam film drainage. *Langmuir* **8**, 3083–3092.

Manning-Benson, S., Bain, C. D. & Darton, R. C. 1997 Measurement of dynamic interfacial properties in an overflowing cylinder by ellipsometry. *J. Colloid Interface Sci.* **189**, 109–116.

Naire, S., Braun, R. J. & Snow, S. A. 2000*a* An insoluble surfactant model for a vertical draining free film. *J. Colloid Interface Sci.* **230**, 91–106.

Naire, S., Braun, R. J. & Snow, S. A. 2000*b* Limiting cases of gravitational drainage of a vertical free film for evaluating surfactants. *SIAM J. Appl. Maths* **61**, 889–913.

Naire, S., Braun, R. J. & Snow, S. A. 2001 An insoluble surfactant model for a vertical draining free film with variable surface viscosity. *Phys. Fluids* **13**, 2492–2502.

Plateau, J. 1873 *Statique Expérimentale et Théorique des Liquides Soumis aux Seules Forces Moléculaires*. Gauthier-Villars.

Schwartz, L. W. & Princen, H. M. 1987 A theory of extensional viscosity for flowing foams and concentrated emulsions. *J. Colloid Interface Sci.* **118**, 201–211.

Shugai, G. 1998 Micromechanics of foam flows. PhD thesis, Stockholm.

Ting, L. & Keller, J. B. 1990 Slender jets and thin sheets with surface tension. *SIAM J. Appl. Maths* **50**, 1533–1546.

Wolfram, S. 1999 *The Mathematica Book*, 4th Edn. Cambridge University Press.